

Gretchen Dykes

Microbial Diversity: Mini-Project Report

## **Irony or coincidence? Exploration of habitats suitable to support chemolithoheterotrophic iron-oxidation.**

### **I. Background**

Fe(II)-oxidizing microbes (FeOM) are an increasingly diverse group of organisms studied for their ability influence availability of heavy metal(loid)s, to enlighten our understanding of earth's history, and even in hopes of generating clean energy via "bio batteries". FeOM by definition oxidize ferrous iron to ferric iron, however this is fraught with quite the challenge since abiotic iron oxidation occurs spontaneously in oxic environments. FeOM must not only compete against abiotic Fe(II)-oxidation, but also generate enough energy for survival.

Several strategies have been described that facilitate proliferation of FeOM. These include growth in low pH environments, growth in micro-oxic environments, and coupling of Fe(II)-oxidation to phototrophy or  $\text{NO}_3^-$  reduction; all of which are reviewed by Melton *et al.* 2014 [1]. While many of the photoferotrophs or  $\text{NO}_3^-$  dependent FeOM have been described as heterotrophs (use of organic substrates as a carbon source), to date to the best of my knowledge, no neutrophilic microaerophilic FeOM have been described as anything other than autotrophs [1-3]. This is surprising in particular due to the established association of neutrophilic lithotrophic FeOB with wetland plant roots that form visible Fe-plaques (amalgamations of Fe-oxides).[4] Plant roots are an excellent source of organic exudates, so it is particularly surprising that organisms using carbon as an electron donor do not out compete the neutro-microaerophiles. Perhaps neutrophilic microaerophilic FeOM are capable of incorporating organic carbon into their biomass, thereby lessening energy loads required for autotrophic carbon acquisition?

My primary project goal was to enrich for possibly heterotrophic FeOM, and to characterize those enriched microbes and their environments. This was achieved by enriching environmental samples from a low redox swamp with heavy detritus loads, worm burrows that create a micro-oxic environment in otherwise anoxic sediment and provide an organic-rich mucus layer, as well as a freshwater stream Fe-mat known to host FeOM. Environments were geochemically characterized, and environmental samples and enrichment samples were characterized according to known Fe-mineral morphologies and taxonomy of known FeOM. Metagenomic data from one of the sample sites was assessed in a preliminary analysis of the microbial community and FeOM it might contain.

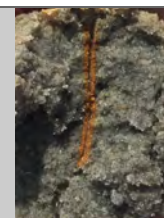
### **II. Methods:**

Samples for enrichment and isolation of FeOB were collected from various locations in Cape Cod, MA (Table 1).

**Table 1: Sample Sites**

Site	pH	dO%	Salinity (ppt)	Conductivity ( $\mu\text{S}/\text{cm}$ )	ORP	Description
Cedar Swamp	5.86	19.2	0.04	77.9	-294.4	Standing water, loaded with detritus, well shaded

School Street Marsh	7.19	35.5	0.15	284.3	-330.5	Fe mat in slow moving creek
Corporate Beach	5.55	44.4	25.19	44051	-296.3	Coastal sediment, oxidized worm burrows



### Enrichment:

For liquid culture enrichment, either 1 mL (mat samples) or 1 g (sediment samples) of sample was inoculated into a 125 mL serum bottle with a N<sub>2</sub> gassed headspace and 50 mL of Minimal Wolfe's Mineral Media (MWMM) for freshwater samples or seawater complete (SWC) for corporate beach samples, amended with vitamin and mineral solutions, 10 mM MES buffered to pH 5.95, 1 mM acetate and approximately 20 mM FeCO<sub>3</sub>. Daily, 4 mL of filtered atmosphere was added to the enrichment to maintain a headspace of approximately 2% oxygen, modified from Emerson & Floyd 2005 [5].

For isolation of FeOB by gradient shake tubes, a 3 mL 2% molten agar plug was prepared in the glovebag with 1.0 mL MWMM and 2.0 mL concentrated FeCO<sub>3</sub>, and allowed to solidify after anoxic autoclaving. The top layer was a 6.0 mL MWMM layer, amended with 1 mM acetate, 1% agar, 10 mM MES buffered to pH 5.95, vitamin and mineral solutions. Either 1 mL (mat samples) or 1 g (sediment samples, prepared in soil slurry) of sample was used as inoculum, and 4, 10-fold serial dilutions were prepared. An oxic headspace was maintained.

### Fluorescence *in situ* hybridization (FISH):

School street marsh and cedar swamp environmental samples, as well as school street marsh and corporate beach enrichments were fixed in 4% formamide for 2 hours at room temperature. Environmental samples were washed twice with phosphate buffered saline solution (PBS) and stored in a 1:1 PBS/ethanol solution at -20 °C. For all samples, 100 µL (environmental samples) or 1 mL (enrichment samples) was diluted in 3 mL PBS and vacuumed onto a 0.2 µM filter. Filters were subsequently rinsed with additional PBS and finally pure water before being embedded in 1% agarose on a microscope slide for storage at room temperature.

Corporate beach worm burrows were stabilized in a 1% agarose gel before fixation, then fixed, as above, in 4% formaldehyde for 2 hours at room temperature, followed by two PBS washes. Burrows were stored at room temperature until individual sand grains visibly coated with Fe-oxides (as indicated by carrot orange color) were selected and placed in a single layer on a 0.2 µM filter. Sand grains sprayed with semi-cooled 1% agarose to ensure stability on the filter for subsequent washes.

All samples were subjected to hybridization with EUB plus Bet42a (and Gam42a inhibitor for  $\gamma$ -proteobacteria) or EUB plus Zeta674 (and ZetaH699, ZetaH722, and ZetaH710 helper probes) in 35% formamide buffer for 2 hrs at 46 °C.[6] Following hybridization, samples were incubated at 48 °C in 35% formamide washing buffer for 20 minutes. Samples were subsequently washed in PBS (10 min, room temperature) and pure water 10 min, room temperature) then stained with DAPI. Samples were visualized by confocal microscopy on Zeiss LSM 800.

### Scanning electron microscopy (SEM):

Sand grains from Corporate Beach and Fe-mat samples from School Street Marsh were fixed in 4% paraformaldehyde overnight at 4 °C. Samples were dehydrated by serial incubation with 25%, 50%, 75%, and finally 100% ethanol for 20 minutes each at room temperature. Critical point drying and platinum sputter coating were completed at the MBL imaging facility prior to visualization with Scanning Electron Microscope Zeiss Supra40VP.

### Cedar Swamp metagenome analysis:

Previously assembled metagenome data from Cedar Swamp was used to generate 31mer and 21mer signatures and compared, using sourmash, to 31mer/21mer signatures from 19 select bacteria and archaea known to use Fe-oxidation in energy generation; (Table 2) according to C. Titus Brown and Luiz Irber's tutorial at:

<https://sourmash.readthedocs.io/en/latest/tutorials.html>. [7] Additionally, Cedar Swamp signatures were compared with signatures of approximately 100,000 sequences in the GenBank database with sourmash.

Assembled metagenome sequence data from Cedar Swamp was binned based on read coverage, coverage variance, and tetranucleotide frequency using MetaBat.[8] Bins were blasted against the NCBI microbial nucleotide database, and results were visualized with VizBin; all according to Lab for Data Intensive Biology tutorial <http://2017-dibsi-metagenomics.readthedocs.io/en/latest/binning.html>. [9]

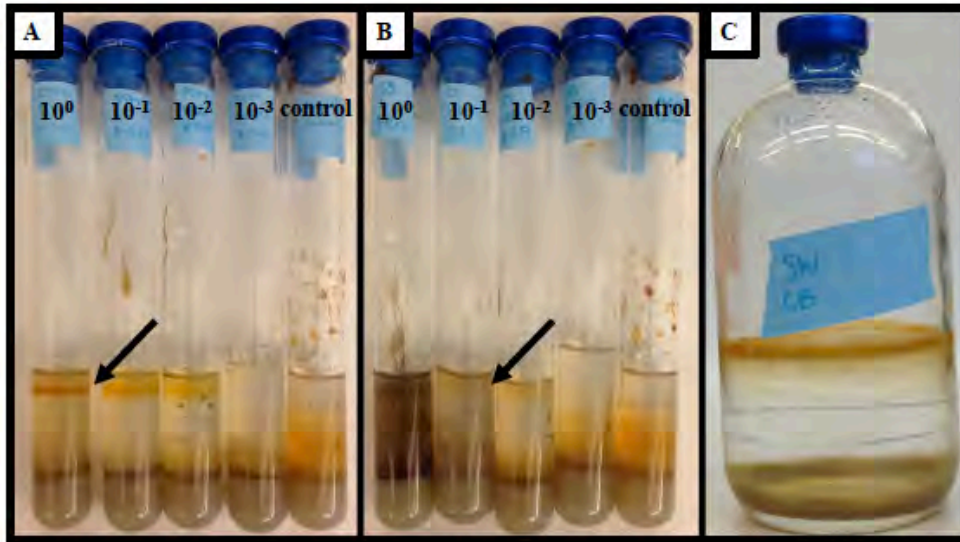
Table 2: Metagenomes of known Fe(II)-oxidizing bacteria and archaea

Genus, species, strain
<i>Thiobacillus denitrificans</i> ATCC 25259
<i>Sideroxydans lithotrophicus</i> ES-1
<i>Rhodopseudomonas palustris</i> TIE-1
<i>Metallosphaera sedula</i>
<i>Mariprofundus ferrooxydans</i> PV-1
<i>Mariprofundus ferrooxydans</i> M34
<i>Marinobacter hydrocarbonoclasticus</i>
<i>Leptothrix cholodnii</i> SP-6
<i>Leptospirillum ferrooxidans</i>
<i>Leptospirillum ferriphilum</i>
<i>Gallionella capsiferiformans</i>
<i>Ferroplasma acidarmanus</i> Fer-1
<i>Ferroglobus placidus</i>
<i>Ferrithrix thermotolerans</i>
<i>Ferrimicrobium acidiphilum</i>
<i>Aquifex aeolicus</i>
<i>Alicyclobacillus ferrooxidans</i> ATCC 232270
<i>Acidimicrobium ferrodidans</i> DMS 10331

### III. Results & Discussion:

#### Enrichments:

Growth (defined as a distinct band of iron oxides) was observed in School Street Marsh shake gradient tubes after three days (pictured after 5 days of growth in Figure 1A). Possible growth appeared in Cedar Swamp shake gradient tubes after 5 days (Figure 1B). Corporate Beach Liquid enrichments displayed evidence of growth as a thin orange iridescent film at the media/headspace interface after 4 days (Figure 1C). Enrichments were transferred to new shake gradient tubes after 5 days of growth. Microbial growth in liquid culture was further investigated with FISH.

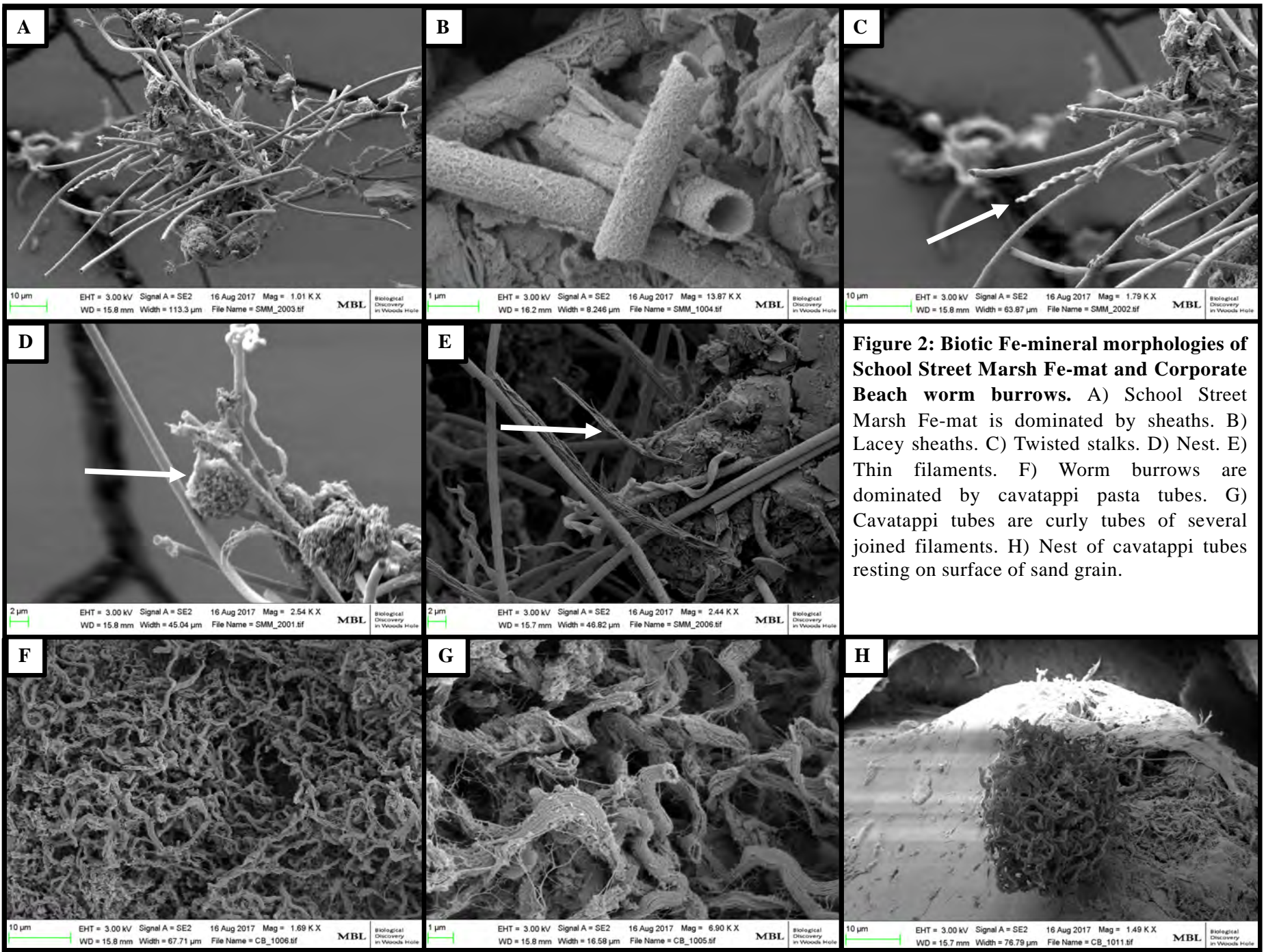


**Figure 1:** Growth of FeOM in gradient shake tubes and liquid media. A) School Street Marsh enrichments developed a fine band of Fe-oxidation (see arrow), indicative of growth of FeOM. B) Cedar Swamp enrichments developed a faint orange band close to the top of the agar plug, which could be indicative of early growth. C) Corporate Beach liquid enrichment developed an iridescent orange film at the media/air interface.

### SEM:

School Street Marsh Environmental Sample:

SEM imaging revealed that the School Street Marsh Environmental Sample was dominated by tube like sheaths (Figure 2A). Sheaths, presumably composed of Fe-oxides, consisted of a lacey lattice, approximately 1  $\mu\text{M}$  in diameter at the opening of the tube (Figure 2B). It should be noted that energy dispersive x-ray analysis was unable to confirm composition of sheath structures. Such sheaths are characteristic of *Leptothrix spp.* and *Sphaerotilus spp.* of the  $\beta$ -proteobacteria, and may be important in preventing total encrustation of the cell in iron-oxide minerals [10]. Also present in the School Street Marsh Sample (Figure 2C) were several instances of twisted stalk Fe-oxide morphology characteristic of the  $\beta$ -proteobacteria *Gallionella ferruginea*, *Ferriphaselus spp.* [10, 11]. Stalk morphologies may serve a chemotaxis-like role in moving the cell towards the ferrous Fe source and away from already oxidized ferric iron. SEM images additionally displayed nests, previously described in a marine Fe- mat by Chan et al. 2014, Figure 2D.[12] Nests were hypothesized to be produced by a cell centered in the nest and to be indicative of secondary colonizers that occupy a geochemical niche lower in  $\text{O}_2$  than sheath and stalk forming primary colonizers.[12] Nests may bear resemblance to previously described *Siderocapsa spp.* capsules, however the nests appear more filamentous than SEM images from Hanert et al. 2006 (though admittedly this may be due to differences in sample preparation/age of mat etc.)[13] It is unknown if the thin, filamentous structures observed



**Figure 2: Biotic Fe-mineral morphologies of School Street Marsh Fe-mat and Corporate Beach worm burrows.** A) School Street Marsh Fe-mat is dominated by sheaths. B) Lacey sheaths. C) Twisted stalks. D) Nest. E) Thin filaments. F) Worm burrows are dominated by cavatappi pasta tubes. G) Cavatappi tubes are curly tubes of several joined filaments. H) Nest of cavatappi tubes resting on surface of sand grain.

in the School Street Marsh have previously been described (Figure 2E), however these structures were conspicuously absent from analysis of a detailed account of marine and freshwater mats.[12] Perhaps these thin filaments are the aged remains of former stalks or sheaths.

#### Corporate Beach:

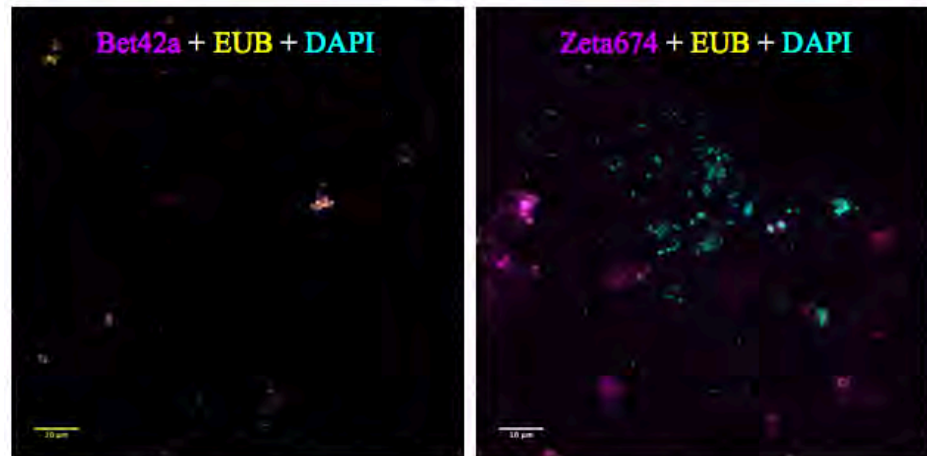
Sand grains imaged from corporate beach hosted what appears to be a less diverse community than that of the School Street Marsh Fe-mat (Figure 2F). Grains were dominated by cavatappi pasta like mineral morphologies (Figure 2G). Cavatappi (presumed) Fe-oxides were just shy of 1  $\mu\text{M}$  in external diameter, appeared to consist of several filaments that formed a tube structure, and curled along the length of the tube. A similar morphology was described by Kato et al. in a marine mat from the Loihi seamount, however curling of the tube was only observed at the mat horizon, at which a shift in geochemical environment likely occurred or in long tubes preceding branching from division. This is in concert with the grain environment, which probably provided a narrow niche for survival of FeOM. Interestingly, cavatappi morphologies were observed flanking the surface of the grain as well as in nest-like balls resting on the surface of the grain (Figure 2H).

#### FISH:

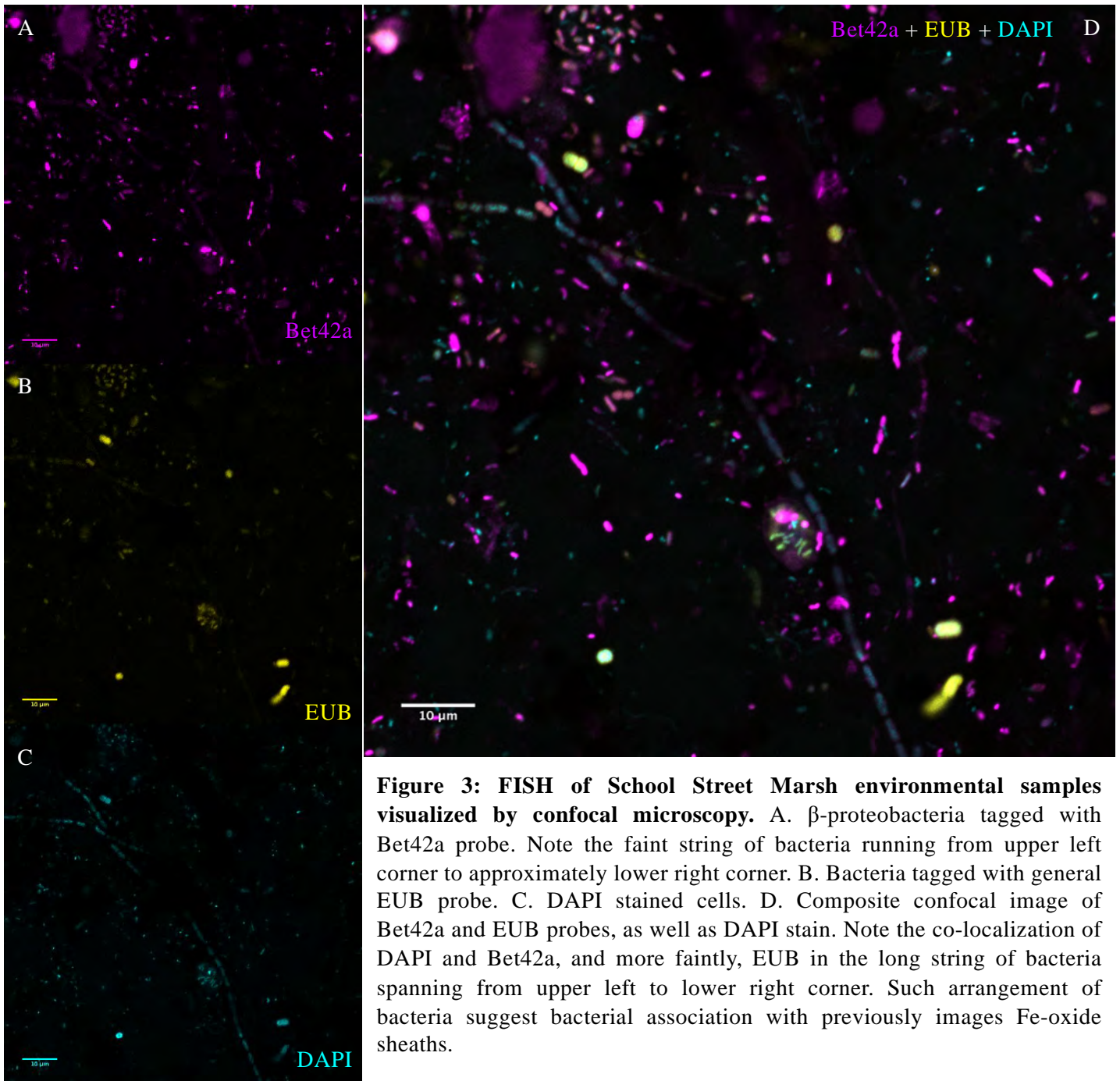
##### School Street Marsh:

A diverse microbial community was observed in the School Street Marsh environmental sample (Figure 3). In several instances, long strings of bacteria presumed to be associated with Fe-oxide sheaths as in Figure # were identified as  $\beta$ -proteobacteria. This supports the hypothesis that these sheath formers may be *Leptothrix spp.* and/or *Sphaerotilus spp.* FeOB. In the School Street Marsh

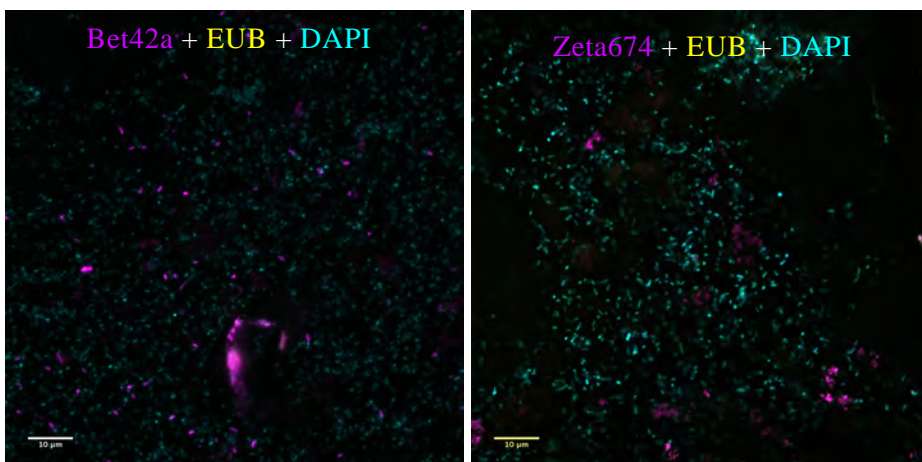
enrichment presence of cells was confirmed by DAPI staining, and was further characterized by FISH (Figure 4). No strings of  $\beta$ -proteobacteria were observed, however the culture did have a higher proportion of  $\beta$ -proteobacteria to all bacteria in comparison to  $\zeta$ -proteobacteria. This was as expected considering the fact that all freshwater neutrophilic microaerophilic FeOM are  $\beta$ -proteobacteria, whereas saltwater neutro-microaerophiles



**Figure 6:  $\zeta$ -proteobacteria and  $\beta$ -proteobacteria are conspicuously absent from Corporate Beach worm burrow enrichments.**  $\zeta$ -proteobacteria and  $\beta$ -proteobacteria (probed with FISH) and total cells (stained with DAPI) were visualized by confocal microscopy. Few  $\beta$ -proteobacteria appear present in the enrichments, and fluorescence from Zeta674 probe does not co-localize with DAPI stain. Lack of co-localization possibly indicates non-specific binding of Zeta674 probes, or perhaps autofluorescence. Both spirilla and bacilli shaped organisms were evident by DAPI stain.

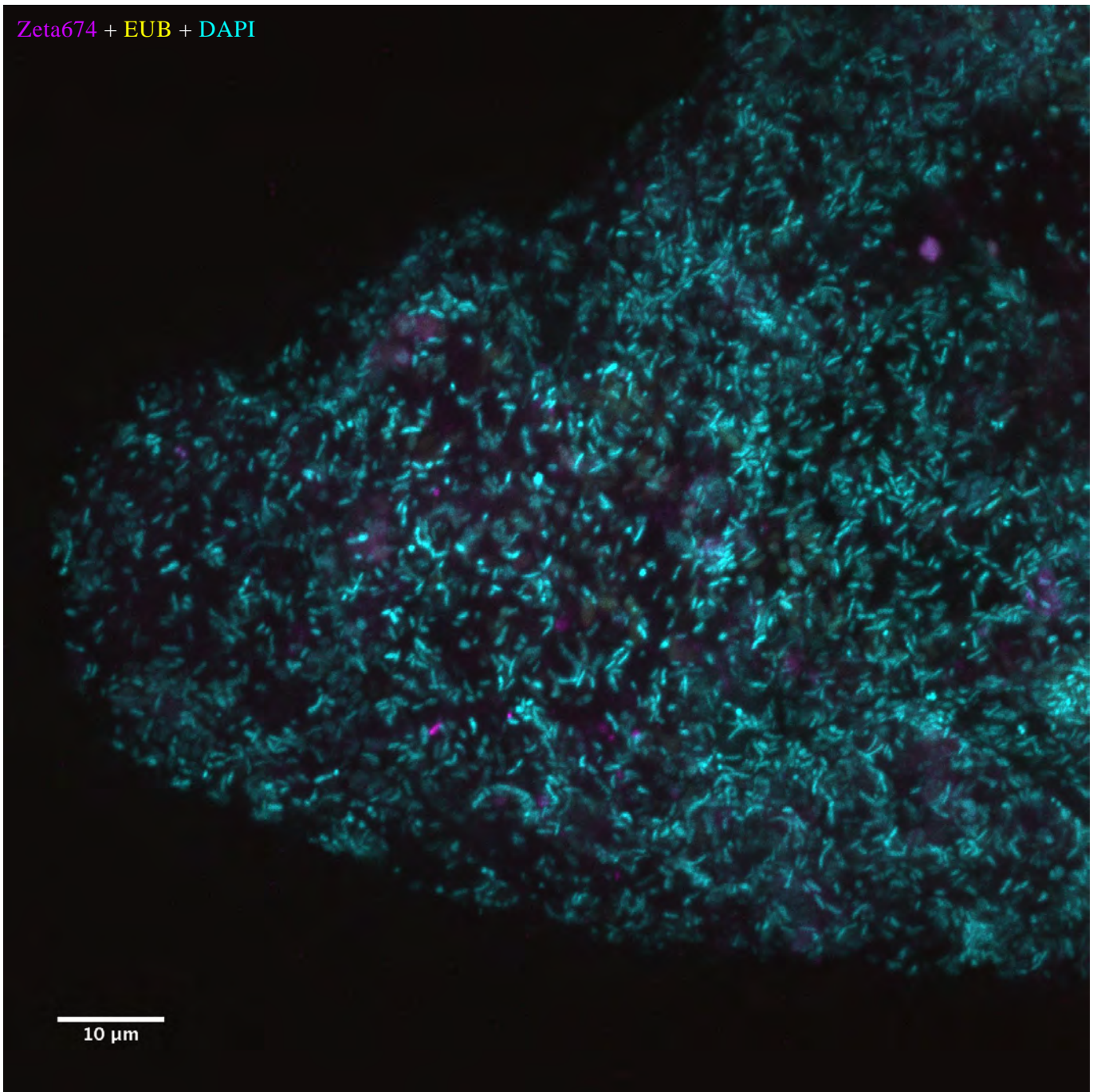


**Figure 3: FISH of School Street Marsh environmental samples visualized by confocal microscopy.** A.  $\beta$ -proteobacteria tagged with Bet42a probe. Note the faint string of bacteria running from upper left corner to approximately lower right corner. B. Bacteria tagged with general EUB probe. C. DAPI stained cells. D. Composite confocal image of Bet42a and EUB probes, as well as DAPI stain. Note the co-localization of DAPI and Bet42a, and more faintly, EUB in the long string of bacteria spanning from upper left to lower right corner. Such arrangement of bacteria suggest bacterial association with previously images Fe-oxide sheaths.



**Figure 4: FISH of School Street Marsh enrichment samples visualized by confocal microscopy.** Samples were collected from liquid cultures 6 days after initial inoculation. Although there appears to be a slightly higher proportion of  $\beta$ -proteobacteria to  $\zeta$ -proteobacteria, the enrichment appears to be heavy with organisms outside these two bacterial groups.

Zeta674 + EUB + DAPI



**Figure 5:  $\zeta$ -proteobacteria and associated microbial community of a Corporate Beach worm burrow sand grain visualized by confocal microscopy.** FISH with Zeta-674 probe targeting  $\zeta$ -proteobacteria revealed a low proportion (compared to total microbes) of this group associated with worm burrow sand grains, despite an abundant microbial community (stained with DAPI, and faintly tagged with EUB probe.) Note the high degree of morphological uniformity of microbes associated with the surface of the sand grain.



are grouped under  $\zeta$ -proteobacteria [10].

**Corporate Beach:**

Surprisingly, few  $\zeta$ -proteobacteria were observed on the surface of sand grains imaged from Corporate Beach worm burrows (Figure 5). The microbial community also appeared to be surprisingly uniform in bacterial morphology, consisting of an abundance of bacilli. Enrichment cultures from Corporate Beach were contrastingly diverse, hosting spirilla and bacilli (Figure 6). Few  $\beta$ -proteobacteria were observed in the enrichment, and presence of  $\zeta$ -proteobacteria remains inconclusive. Since expected probe fluorescence did not co-localize with DAPI it is possible that auto-fluorescence or non-specific probe binding occurred.

Autofluorescence and extreme sparsity of microbes in Cedar Swamp environmental samples prevented adequate analysis by FISH.

**Cedar Swamp metagenome analysis:**

No signature similarities were found between the Cedar Swamp metagenome and the metagenomes of the 19 known FeOM for either 31mer or 21mer analysis.

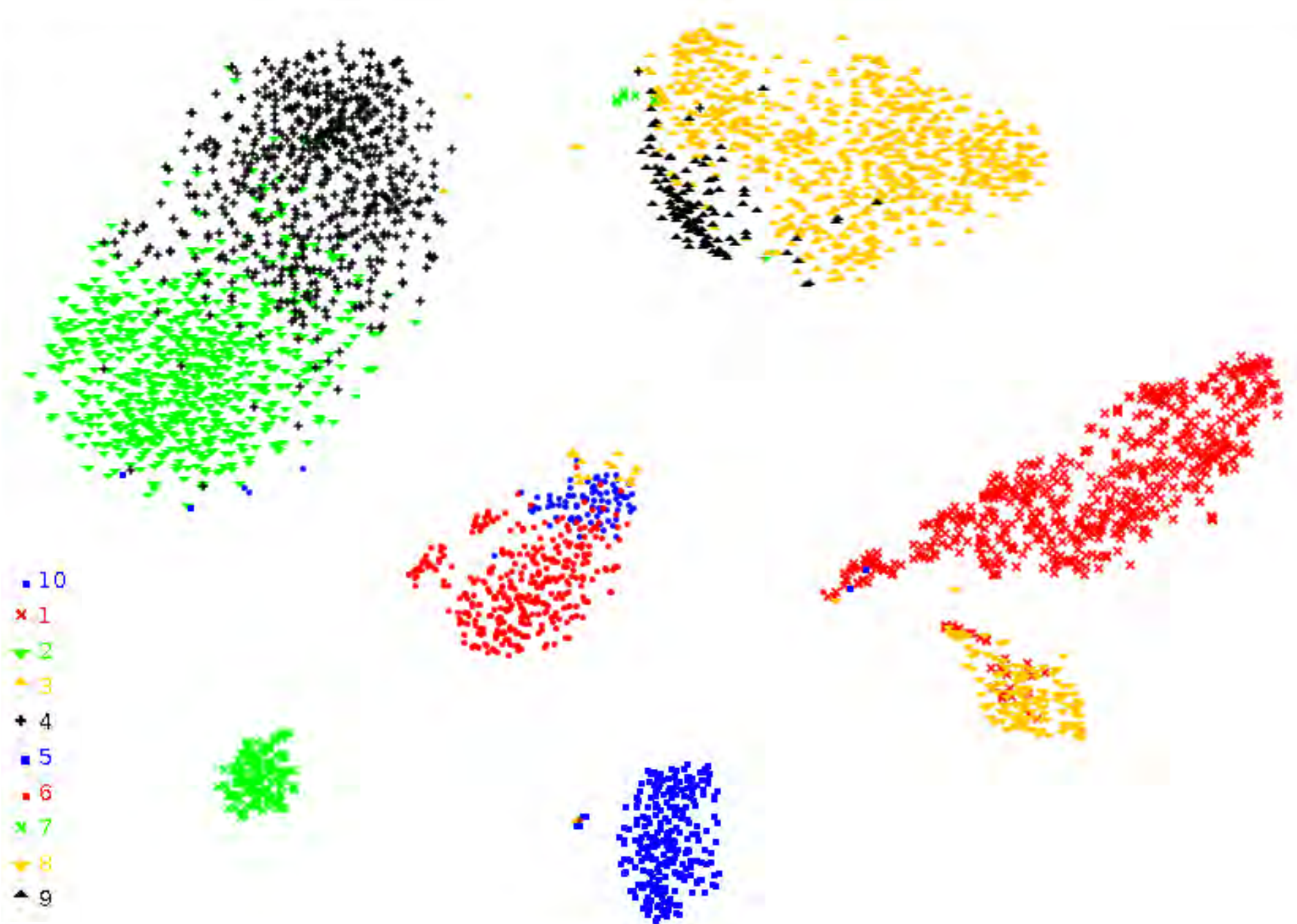
For the 31mer signature analysis, only six matches were recovered from the GenBank database (Table 3), hitting only 0.2% of the Cedar Swamp signature. These matches had very little base pair overlap with Cedar Swamp signatures.

**Table 3: 31mer signature analysis of Cedar Swamp Metagenome**

Overlap (kbp)	p_query	p_match	GenBank Accession	Name
170.0	0.1%	1.9%	LT670818.1	<i>Bradyrhizobium erythrophlei</i> strain GAS242
90.0	0.0%	3.6%	CGYF01000001.1	<i>Streptococcus pneumoniae</i>
70.0	0.0%	0.7%	AUGA01000001.1	<i>Bradyrhizobium sp. th.b2</i>
80.0	0.0%	1.6%	FACE01000001.1	<i>Peptoclostridium difficile</i> isolate VL_0117
50.0	0.0%	0.7%	JZWI01000001.1	<i>Variovorax paradoxus</i> strain TBEA6
80.0	0.0%	0.8%	LNEC01000001.1	<i>Bradyrhizobiaceae</i> bacterium Ga0074131

Binning by MetaBat yielded 10 bins. BLAST results for bins are reported in Table #. Although BLAST results had high identity to binned contigs, all resulted in a coverage of less than 27% of the contigs. Although this could indicate that the bins represent previously unsequenced microbes, it is more likely that low sequence coverage contributed to poor binning which limited sequence data within those bins from which to infer taxonomy. Future analysis would benefit from a bin analysis such as CheckM, which can be used to infer quality of binning.

Visualization of bins by VizBin yielded clusters with moderate differences compared to MetaBat binning (Figure 7). Whereas MetaBat binned contigs into 10 bins, 7 distinct clusters are discernable in the VizBin scatterplot, which displays differences between genomic signatures of contigs in a 2D format so as to allow the viewer to visually determine bins or clustering of contigs.[9] Comparison of VizBin clusters to MetaBat bins revealed stark differences regarding


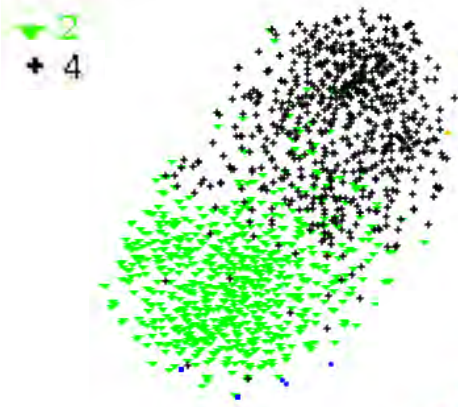


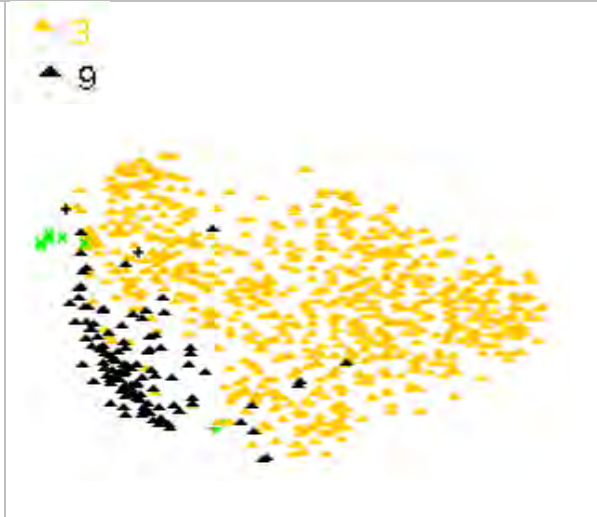
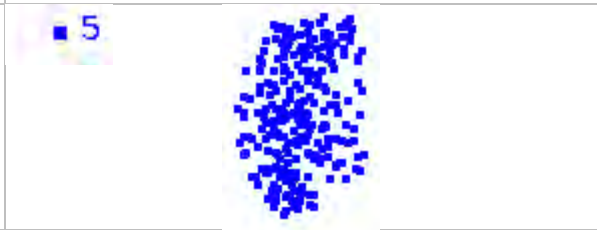
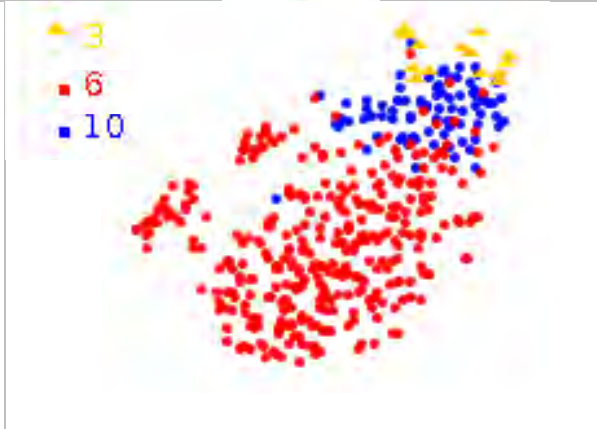


**Figure 7: Visualization of MetaBat bins by VizBins.** Contigs (individual points) are colored according to MetaBat bin number (legend above). Several instances of discrepancies between bins and clusters are apparent.

BLAST hits (Table 4). This could be due to the difference in binning methodology, or once again to lack of depth of sequencing in this likely diverse community. Interestingly, one cluster shares similarity between MetaBat and VizBin. The VizBin cluster that encompasses contigs from MetaBat bins 3, 6, and 10 was identified by a BLAST nucleotide search to be *Opitutus terrae* PB90-1. Promisingly, this match covered a whopping 27% percent of the search query, the highest of any bins or clusters. The MetaBat bin 6 also matched to *Opitutus terrae* PB90-1, covering 27% of the query. This indicates that this MetaBat bin and VizBin cluster were at least partially successful in grouping several contigs belonging to the same organism.

Overall, it seems that issues with bioinformatics analysis may stem from the dataset itself. The raw dataset contained 34,851,570 reads obtained from MiSeq paired-end sequencing (2x150) for a total of 10.455 Gbp. This number of reads is rather low, considering that high quality data sets fall in the range of hundreds of millions of reads (cite Titus’s pre print). Additionally, assembly analysis by Quast revealed an N50 score of only 803. Ultimately, deeper sequencing of this evidently diverse microbial community would improve assembly of this dataset and would therefore allow for better understanding of the Cedar Swamp microbial community that are present in Cedar Swamp.

**Table 4: Comparison of MetaBat bins and VizBin clusters**

MetaBat Query Cover	MetaBat Group Taxonomy	MetaBat & VizBin Bin Identity	VizBin Group Taxonomy	VizBin Query Cover
1%	<i>Gordonibacter</i> sp. Marseille-P2775		<i>Halococcus sediminicola</i> CBA1101	2%
2: 4: 0%	2: No significant sequence similarity found  4: <i>Pseudomonas fluorescens</i> L111		<i>Burkholderia glebae</i> LMG 29325, <i>Caballeronia glathei</i> DSM 50014, <i>Caballeronia zhejiangensis</i> strain OP-1, <i>Burkholderia concitans</i> LMG 29315	1% (all)

<p>3: 9: 1%</p>	<p>3: No significant sequence similarity found</p> <p>9: <i>Pseudomonas fluorescens</i> L111</p>		<p><i>Halococcus sediminicola</i> strain CBA1101</p>	<p>1%</p>
	<p>No significant sequence similarity found</p>		<p>No significant similarity found</p>	
<p>3: 6: 14% 10: 27%</p>	<p>3: No significant sequence similarity found</p> <p>6: <i>Solibacter usitatus</i> Ellin6078</p> <p>10: <i>Opitutus terrae</i> PB90-1</p>		<p><i>Opitutus terrae</i> PB90-1</p>	<p>27%</p>
	<p>No significant similarities found</p>		<p>No significant similarity found</p>	
<p>1: 1% 8: 1%</p>	<p>1: <i>Gordonibacter</i> sp. Marseille-P2775</p> <p>8: <i>Pseudomonas fluorescens</i> L321</p>		<p>No significant similarity found</p>	

#### IV. References:

1. Melton, E.D., et al., *The interplay of microbially mediated and abiotic reactions in the biogeochemical Fe cycle*. Nature Reviews Microbiology, 2014. **12**(12): p. 797-808.
2. Caiazza, N.C., D.P. Lies, and D.K. Newman, *Phototrophic fe(II) oxidation promotes organic carbon acquisition by Rhodobacter capsulatus SB1003*. Applied and Environmental Microbiology, 2007. **73**(19): p. 6150-6158.
3. Kappler, A., B. Schink, and D.K. Newman, *Fe(III) mineral formation and cell encrustation by the nitrate-dependent Fe(II)-oxidizer strain BoFeN1*. Geobiology, 2005. **3**(4): p. 235-245.
4. Emerson, D., J.V. Weiss, and J.P. Megonigal, *Iron-oxidizing bacteria are associated with ferric hydroxide precipitates (Fe-plaque) on the roots of wetland plants*. Applied and Environmental Microbiology, 1999. **65**(6): p. 2758-2761.
5. Emerson, D. and M.M. Floyd, *Enrichment and isolation of iron-oxidizing bacteria at neutral pH*, in *Environmental Microbiology*, J.R. Leadbetter, Editor. 2005. p. 112-123.
6. Fleming, E.J., et al., *Hidden in plain sight: discovery of sheath-forming, iron-oxidizing Zetaproteobacteria at Loihi Seamount, Hawaii, USA*. Fems Microbiology Ecology, 2013. **85**(1): p. 116-127.
7. Brown, T.C., Irber, L., *sourmash: a Library for {MinHash} sketching of {DNA}*. The Journal of Open Source Software, 2016. **1**(5).
8. Kang DD, F.J., Egan R, Wang Z. , *MetaBAT, an efficient tool for accurately reconstructing single genomes from complex microbial communities*. PeerJ, 2015. **3**(e1165).
9. Laczny, C.C., et al., *VizBin - an application for reference-independent visualization and human-augmented binning of metagenomic data*. Microbiome, 2015. **3**.
10. Emerson, D., E.J. Fleming, and J.M. McBeth, *Iron-Oxidizing Bacteria: An Environmental and Genomic Perspective*, in *Annual Review of Microbiology, Vol 64, 2010*, S. Gottesman and C.S. Harwood, Editors. 2010. p. 561-583.
11. Kato, S., et al., *Ferriphaseelus amnicola gen. nov., sp nov., a neutrophilic, stalk-forming, iron-oxidizing bacterium isolated from an iron-rich groundwater seep*. International Journal of Systematic and Evolutionary Microbiology, 2014. **64**: p. 921-925.
12. Chan, C.S., et al., *The Architecture of Iron Microbial Mats Reflects the Adaptation of Chemolithotrophic Iron Oxidation in Freshwater and Marine Environments*. Frontiers in Microbiology, 2016. **7**(796).
13. Hanert, H.H., *The prokaryotes*. 2 ed. The genus Siderocapsa (and other iron-and manganese-oxidizing eubacteria), ed. S.N. York. Vol. IV. 2006.